Eye (2014) 28, 26–33

www.nature.com/eye

CLINICAL STUDY

Ophthalmic manifestations in a Chinese family with familial amyloid polyneuropathy due to a TTR Gly83Arg mutation

T Liu[1,2,8], B Zhang[3,8], X Jin[1,8], W Wang[4], J Lee[5], J Li[6], H Yuan[7] and X Cheng[3]

[1]Department of Ophthalmology, Chinese PLA General Hospital, Beijing, China

[2]Department of Ophthalmology, Hainan Branch of Chinese PLA General Hospital, Sanya, China

[3]Department of Ophthalmology, Chinese PLA Medical School, Beijing, China

[4]Department of Gastroenterology and Hepatology, Hainan Branch of Chinese PLA General Hospital, Sanya, China

[5]Department of Ophthalmology and Shiley Eye Center, University and California San Diego, La Jolla, California, USA

[6]Collage of life Science, Nankai University, Tianjin, China

[7]Institute of Otolaryngology, Chinese PLA General Hospital, Beijing, China

Correspondence:
T Liu, Department of Ophthalmology, Chinese PLA General Hospital, 28 Fuxing Road, Beijing 100853, China.
Tel: +86 10 68187998;
Fax: +86 10 68187998.
E-mail: ltc301@sina.com
[8]These authors contributed equally to this work.

Received: 2 April 2013
Accepted in revised form: 4 September 2013
Published online: 11 October 2013

Abstract

Purpose **To describe the characteristic ophthalmic phenotypes of a large Chinese family with familial amyloid polyneuropathy due to a missense mutation in transthyretin (*TTR*) (c.307 C>G).**

Methods **Twenty-seven individuals (12 affected, 15 unaffected) from a five-generation Chinese family underwent general medical examination and comprehensive ophthalmic examination, including best correct visual acuity, intraocular pressure measurements, Schirmer test, slitlamp examination, fundoscopy, and ocular ultrasonography. Histological examination of vitreous biopsies using Congo red staining and immunohistochemistry was performed. Cardiovascular magnetic resonance (CMR), electrocardiogram, and echocardiogram were used to evaluate cardiac amyloidosis. Electromyography was used to evaluate nerve function. All four exons of *TTR* were amplified by PCR, sequenced using a Bigdye terminator v3.1 cycle sequencing kit and analyzed on an ABI 3700XL Genetic Analyzer.**

Results **All 12 affected individuals in the family had ocular manifestations, including severe vitreous opacities, secondary glaucoma, xerophthalmia, dyscoria, and attenuated retinal arteries. Congo red staining demonstrated amyloid deposits in the vitreous, and immunohistochemical staining confirmed the deposition of TTR proteins in the vitreous. Twelve individuals had polyneuropathy, and electromyography detected functional damage in peripheral nerves. One individual was diagnosed with cardiac amyloidosis by CMR. Direct sequencing revealed the heterozygous missense mutation in *TTR* (c.307 C>G p.Gly83Arg) in all 12 affected individuals. The mutation co-segregated with the disease phenotype and was absent in 100 normal controls.**

Conclusions **Vitreous opacity is very common in patients with the TTR Gly83Arg mutation; other clinical characteristics associated with the mutation include polyneuropathy and cardiac amyloidosis.**

Eye (2014) **28,** 26–33; doi:10.1038/eye.2013.217; published online 11 October 2013

Keywords: familial amyloid polyneuropathy; transthyretin; mutation; Gly83Arg; vitreous; Chinese

Introduction

Familial amyloid polyneuropathy (FAP) is a group of autosomal dominant inherited disorders characterized by protein fibril deposition in multiple organs, leading to physiologic dysfunction.[1] Typical clinical manifestations of FAP include polyneuropathy, carpal tunnel syndrome, autonomic insufficiency, cardiomyopathy, and gastrointestinal dysfunction, occasionally accompanied by vitreous opacities and renal insufficiency.[2] The incidence of FAP varies greatly, and several regional clusters have been identified.[3]

FAP can be classified into three main types according to the amyloid precursor protein: transthyretin (TTR), apolipoprotein A-I, and gelsolin.[4] Mutations in TTR are the most common cause of FAP, and more than 100 pathogenic variants of TTR have been reported. TTR is a normal serum protein synthesized

mainly in the liver (90%) and it is also produced locally by the choroid plexus in the brain and the retinal pigment epithelial cells in the eye.[5–10]

TTR Val30Met mutation is the most common pathogenic variant overall and in Portugal, Brazil, Sweden, and Japan, and TTR Val122Ile is the most common pathogenic variant in the United States.[4,11] In China, only six pathogenic TTR variants (Gly54Arg, Gly83Arg, Lys35Thr, Leu55Arg, Val30Ala, Y114C) have been reported, and hot spots of *TTR* mutations have not yet been identified.[12–17]

Here, we describe the clinical manifestations, management, and long-term follow-up of a large Chinese family with a heterozygous missense mutation in TTR Gly83Arg (c.307 C>G).

Subjects and methods

This study was approved by the Ethical Review Board of the Chinese PLA General Hospital and adheres to the tenets of the Declaration of Helsinki. Informed consents were signed by all participants, and in cases involving minors, informed consents were signed by their parents. Twenty-seven subjects (12 affected individuals and 15 unaffected individuals) from a five-generation Chinese family (Figure 1a) and hundred normal controls were included in the study. The controls were randomly selected from the outpatient department of the Chinese PLA General Hospital and consisted of subjects greater than 50 years of age without visual impairments and vitreous opacity confirmed by indirect ophthalmoscope. Individuals with systemic diseases or personal or family history of known inherited disease were excluded. A retrospective chart review of nine deceased individuals in the family was also performed.

The family in this study was identified and clinically followed in the Chinese PLA General Hospital. All 27 participants underwent a thorough medical history and general examination, routine blood work (complete blood count, chemistry panel), electrocardiogram, and abdominal ultrasonography. Additional tests, including electromyography, echocardiogram, cardiovascular magnetic resonance (CMR) with gadolinium enhancement. Comprehensive ocular examinations, including best correct visual acuity, intraocular pressure (IOP) measurements, Schirmer test, slitlamp examination, three-mirror lens, and fundoscopic examinations were performed on all 27 subjects in this family. In addition, ocular ultrasonography and ultrasound biomicroscopy (UBM) were performed in patients IV:4, IV:6, and IV:8. All results and images were interpreted by an experienced specialist.

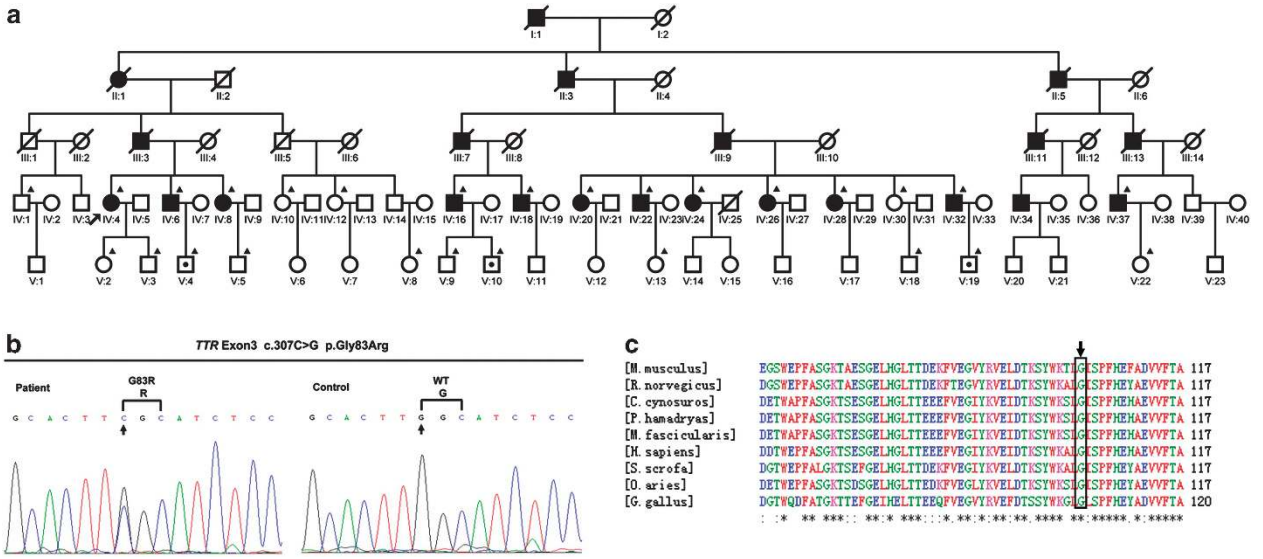

Figure 1 (a) The Pedigree of the family with FAP. I: first generation, II: second generation, III: third generation, IV: fourth generation, V: fifth generation. Arrow: the proband. Filled symbols: affected individuals. Slashed symbols: deceased individuals. Solid triangle: the individuals who underwent clinical and genetic analyses. Black dot: asymptomatic individuals with the TTR Gly83Arg. (b) The *TTR* sequencing results. Sanger sequencing of exons of *TTR* data shows that a G to C transversion (arrow) resulted in the substitution of glycine-83 by arginine (Gly83Arg) in affected individuals of the family. The corresponding normal sequence (arrow) was found in unaffected family members and controls. (c) Multiple sequence alignment of TTR. Sequence alignment of TTR from nine species is shown. Gly83 occurs at a highly conserved position in TTR (arrow). The evolutionary conservativity of TTR is indicated using asterisk (highly conservative), colon (less conservative) and dot (poorly conservative).

Histological examinations

Histological examinations were performed on 4-μm sections of formalin-fixed paraffin-embedded vitreous biopsies obtained during vitrectomies from patients IV:4 and IV:6. Vitreous biopsies were stained with Congo red and analyzed with polarized light to check for green birefringence.[18] Immunohistochemical staining was performed using a rabbit anti-human TTR polyclonal antibody (Sigma, St Louis, MO, USA; HPA002550), with streptavidin-biotin-peroxidase as the detection system and diaminobenzidine as chromogen.[19] Cytoplasmic staining of human pancreas islet cells was used as positive control and absence of TTR polyclonal antibody was used as negative control.

Molecular genetic analysis

Genomic DNA isolated from peripheral leukocytes was obtained from all 27 participants in the family and 100 controls using the TIANamp Blood DNA Kit (Tiangen Biotech Co. Ltd, Beijing, China). All coding exons of *TTR* were amplified by PCR using a set of four pairs of primers, which were designed using Primer3 software (http://frodo.wi.mit.edu/primer3/). Twenty five μl volumes containing 50 ng genomic DNA, 5 pmol l^{-1} of each primer, 2 mmol l^{-1} $MgCl_2$, 5 nmol l^{-1} deoxyribonucleotide triphosphate, PCR buffer provided by the manufacturer, and 0.5 U of Taq polymerase (Tiangen Biotech Co. Ltd) were used for PCR reaction. The PCR reactions were performed as follows: denaturation at 94 °C for 3 min, followed by 30 cycles of 94 °C for 30 s, annealing at 55 °C for 30 s, and elongation at 72 °C for 1 min, ending with a final extension step of 72 °C for 5 min. The PCR products were sequenced using a Bigdye terminator v3.1 cycle sequencing kit (ABI, Foster City, CA, USA) and analyzed on an ABI 3700XL Genetic Analyzer.

Results

Participants

The Chinese family in this study was from Guizhou province in southwest China. There were 85 individuals in the five-generation pedigree with 22 affected individuals (13 living, 9 deceased; Figure 1a). Detailed clinical data and peripheral blood samples were obtained from 27 subjects (12 affected individuals and 15 unaffected individuals). Twelve affected individuals had ocular manifestations, polyneuropathy, and cardiomyopathy, supporting the diagnosis of FAP. Clinical manifestations consistent with FAP were present in individuals in the first four generations of the family. The ratio of affected males to females was approximately 2.5 : 1, which was consistent with an autosomal dominant pattern of inheritance.

Systemic manifestations

The clinical characteristics of the 12 affected individuals are summarized in Table 1. Routine blood workup, which included a complete blood count and chemistry panel, were within normal limits and no abnormalities of the liver and kidney were found on ultrasonography in all 12 affected individuals.

Ten affected individuals had peripheral neuropathy starting in the upper extremities with symptoms of numbness and tingling in the fingers and thenar muscle paralysis. Motor dysfunctions were found in four patients. IV:16 and IV:18 initially had severe pain in the lower extremities and IV:16 subsequently developed

Table 1 Clinical characteristics of affected family members

Pedigree ID	*Sex*	*Age (years)*	*Initial manifestation*	*Age of disease onset (years)*	*Organs affected*			
					Eye	*Peripheral nerve system*		*Heart*
						Upper extremities	*Lower extremities*	
IV:4	F	58	VO	41	Yes	Yes	No	No
IV:6	M	50	VO	38	Yes	Yes	Yes	Yes
IV:8	F	45	VO	40	Yes	Yes	No	No
IV:16	M	52	VO	44	Yes	Yes	Yes	No
IV:18	M	48	VO	42	Yes	Yes	Yes	No
IV:20	F	59	P	37	Yes	Yes	No	No
IV:22	M	58	VO	39	Yes	Yes	No	No
IV:24	F	57	VO	43	Yes	Yes	No	No
IV:26	F	52	VO	42	Yes	Yes	No	No
IV:28	F	47	VO	41	Yes	No	No	No
IV:32	M	42	VO	41	Yes	No	No	No
IV:37	M	51	VO	47	Yes	Yes	Yes	No

Abbreviations: F, female; M, male; P, polyneuropathy; VO, vitreous opacity.

paralysis of the lower extremities. Patients IV:4, IV:6, and IV:8 underwent electromyography, and the results showed a diffuse axonal sensorimotor peripheal neuropathy with median nerve lesion at wrist of upper limbs, and decreased nerve conduction velocities of the median, ulnar, and radial nerves. In patient IV:6, the result showed a neurogenic pattern in the extremities supported by that the velocity and compound muscle action potential amplitude of the median, peroneus, and tibial nerve as well as sensory conduction velocity and sensory action potiential amplitude of the median and radial nerve could not be detected.

Of all subjects in the study, only patient IV:6 had evidence of cardiac amyloidosis on ECG and echocardiogram, which demonstrated left ventricular hypertrophy and atrioventricular block; and mildly thickened left ventricular wall and impaired systolic and diastolic function, respectively. CMR demonstrated diffuse myocardial enhancement after gadolinum delivery, indicating diffuse amyloidosis in the myocardium.[20]

Ophthalmic manifestations

The initial symptom in 11 of the 12 (91.7%) affected individuals was visual floaters or vision loss secondary to vitreous opacities. The twelfth patient (IV:20) reported numbness in the upper extremities as the initial symptom. Other ocular manifestations included secondary glaucoma, xerophthalmia, dyscoria, and slow response to tropicamide (Table 2). Numerous cotton wool-like deposits in the vitreous were revealed on fundoscopy (Figure 2a) and large mass in the peripheral vitreous was detected in patients with incomplete vitrectomy (Figure 2b), showing strong echo by ocular ultrasonography (Figure 2c). In some patients, amyloid deposits in peripheral vitreous were found to be sheet-like during vitrectomy (Figure 2d). Fundoscopy also revealed attenuated retinal arteries and whitish deposits on retinal arterioles (Figure 2e). It was found by slit lamp that the deposits attached to the posterior lens capsule, resembling footplates (Figure 2f). Schirmer test showed decreased lacrimal secretion in 10 patients (Table 2). The mydriatic response time after tropicamide application was greater than 1.5 h in nine patients, and scalloped pupils during mydriasis was noted in two patients (IV:8 and IV:18; Figure 2g).

0.5–2 years after the onset of floaters, the vitreous opacity gradually worsened, resulting in significantly impaired visual acuity. Twenty-one eyes in 11 affected individuals underwent incomplete vitrectomies and visual acuity improved in all eyes. Lens opacity was graded according to lens opacities classification system II (Table 2). We found that five years (range from 1 month to 11 years) after incomplete vitrectomy without posterior vitreous detachment (PVD), lens of 15 eyes in nine patients were still clear (Figure 2f). Only six lenses in four patients became opaque and two intraocular lenses were implanted in two patients. Seven to ten years after the first operation, a second vitrectomy was performed in four eyes of three patients (IV:4, IV:6, and IV:26) because amyloid continued to deposit in the residual vitreous in the posterior pole and periphery, resulting in severe visual impairment. Vitreous

Table 2 Ocular manifestations of affected individuals in the family

Pedigree ID	*Surgical procedure*	*BCVA (OD/OS)*		*Current lens status LOCS II (OD/OS)*	*Current IOP (mm Hg) (OD/OS)*	*Schimer test (mm) (OD/OS)*	*Mydriasis after tropicamide administration*		*Age of disease onset (years)*		*Other ocular findings*		
		Baseline	*Final*				*Mydriasis time (min)*	*Dyscoria*	*Vitreous opacity*	*Glau coma*	*Pale optic disc*	*Attenuated retinal arterioles*	*Whitish deposits*
IV:4	Vitre, Cycloph	0.04/0.1	0.8/0.5	N1/IOL	24/31	5/2	30	Nor	41	47	Yes	Yes	Yes
IV:6	Vitre, Treb Cycloph	HM/HM	HM/FC	N1/N2	12/34	0/4	>90	Nor	38	49	Yes	Yes	Yes
IV:8	Vitre	0.06/FC	1.0/0.8	N1/N1	18/16	7/5	30	Scalloped	40	NA	No	No	Yes
IV:16	Vitre	HM/FC	0.2/FC	N1/N1	14/17	3/7	>90	Nor	44	NA	No	Yes	Yes
IV:18	Vitre	FC/FC	0.6/0.5	N1/N1	14/18	0/5	>120	Scalloped	42	NA	No	No	No
IV:20	Vitre, Treb	FC/FC	LP/0.4	N4/IOL	45/33	0/0	>120	Nor	42	50	Yes	Yes	Yes
IV:22	Vitre	FC/LP	0.15/LP	N1/[a]	17/18	0/0	>120	Nor	39	NA	No	Yes	Yes
IV:24	Vitre, Treb	0.04/FC	0.1/NLP	N4/N4	51/54	3/0	>120	Nor	43	51	Yes	Yes	Yes
IV:26	Vitre	FC/0.06	FC/0.8	N1/N1	17/18	12/10	>120	Nor	42	NA	No	Yes	Yes
IV:28	Vitre	FC/FC	0.5/0.8	N1/N1	14/15	10/7	>90	Nor	41	NA	No	No	No
IV:32	None	HM/1.2	HM/1.2	N1/N1	15/17	0/9	>90	Nor	41	NA	No	No	No
IV:37	Vitre	FC/FC	0.4/0.5	N1/N1	16/17	2/7	30	Nor	47	NA	No	Yes	No

Abbreviations: BCVA, best correct visual acuity; Cycloph, cyclophotocoagulation; FC, finger counting; HM, hand movement; IOL: intraocular lens; IOP, intraocular pressure; LOCS II, lens opacities classification system II; LP, light perception; NA, not applicable; Nor, normal; OD, right eye; OS, left eye; NLP, no light perception; Treb, trabeculectomy; Vitre, vitrecotmy. In LOCS II, lens nuclear sclerosis was classified as trace (N1), mild (N2), moderate (N3), and severe (N4).
Note: Visual acuity before and after surgery were recorded as baseline and final one.
[a]The len could not be seen because of traumtic corneal leucoma.

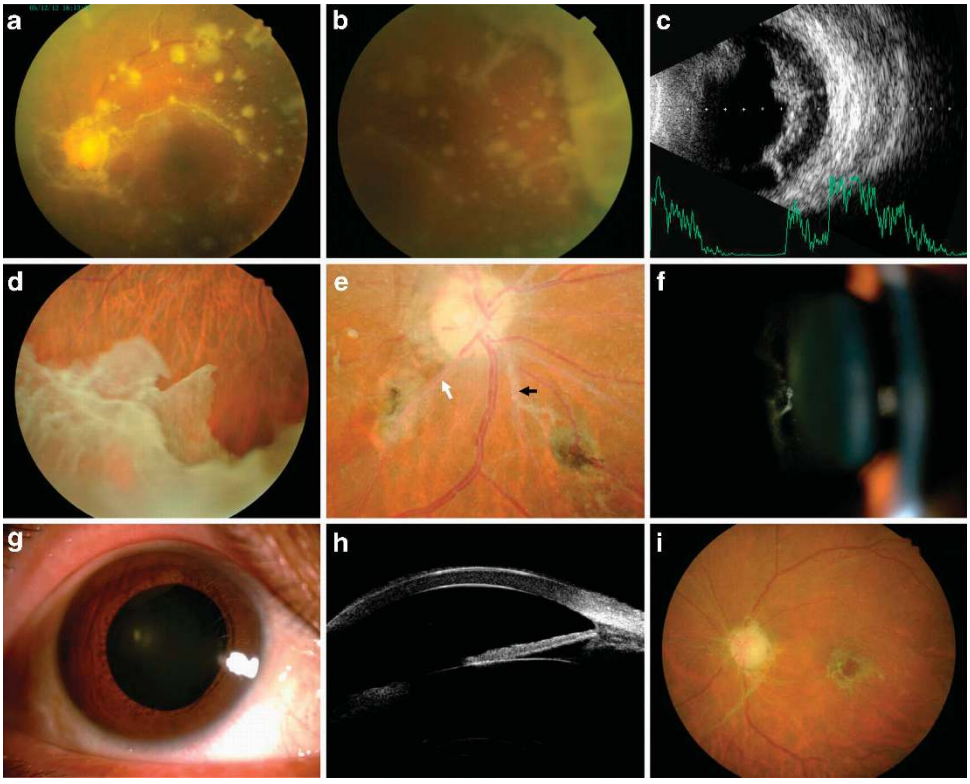

Figure 2 Ophthalmic features in patients with FAP. (a) Fundus photography showed numerous yellow-white, lump, cotton wool-like deposits in the vitreous. (b) A large dense peripheral vitreous was observed and (c) it was showed strong echo by ocular ultrasongraphy. (d) After vitrectomy, the residual sheet-like deposits in peripheral vitreous were observed. (e) The attenuated retinal artery (white arrow) and the whitish deposits along the small retinal arterioles were observed (black arrow), which seemed to emanate from the blood vessels. (f) The deposits attached to the posterior lens capsule, which looked like footplates. (g) During mydriatsis, scalloped pupils were observed. In patients with secondary glaucoma, UBM showed open anterior chamber angles (h) and fundoscopy revealed a pale optic nerve (i).

amyloidosis in the posterior pole adhered to the retina so strongly that it was difficult to induce a PVD during the operation. After surgery, visual acuity improved significantly in patients IV:4 and IV:26, but not in patient IV:6 who suffered from glaucoma in both eyes.

Glaucoma was diagnosed in both eyes of four patients approximately 6–10 years after the onset of disease. UBM showed open anterior chamber angles (Figure 2h) and fundoscopy revealed a pale optic nerve (Figure 2i). These four patients all had elevated IOP with the highest IOP being 54 mm Hg. The IOP could not be lowered to normal ranges with multiple IOP-lowering drugs. Trabeculectomy initially lowered the IOP of these patients to normal ranges, but the IOP increased to 30–35 mm Hg 3 months after treatment. Subsequently, two patients had to undergo cyclophotocoagulation and IOP was successfully controlled.

Mutation analysis

Sequence analysis of *TTR* revealed a heterozygous missense mutation in exon 3 (c.307 C>G) in the 12 affected patients as well as 3 asymptomatic individuals whose age is within 12–23 years. This mutation (c.307C>G) resulted in a transition in the coding sequence, changing the GGC codon for glycine to a CGC codon for arginine (Gly83Arg). This mutation was absent in 100 unrelated normal controls (Figure 1b).

Conservation of TTR Gly83

We screened *TTR* orthologs using the NCBI HomoloGene database. (http://www.ncbi.nlm.nih.gov/sites/entrez?cmd=Retrieve&db=homologene&dopt=MultipleAlignment&list_uids=5859), which revealed that Gly83 was highly conserved among multiple species (Figure 1c).

Congo red staining and immunohistochemistry

Vitreous biopsy from two affected individuals (IV:4 and IV:6) stained positive with Congo red and showed apple-green birefringence under polarized light with widespread deposition of amyloid in the vitreous.

Positive immunohistochemical staining of TTR in the vitreous samples confirmed the presence of TTR proteins in the vitreous.

Structure modeling of TTR Gly83Arg

Homology modeling of the TTR Gly83Arg mutant and retinol-binding protein (RBP) complex was made by employing the high-resolution X-ray structure of the wild-type TTR and RBP complex as the template, through the SWISS-MODEL server to build the optimized three-dimensional atomic representations.[21]

TTR is a homo tetrameric protein with each subunit composed of 127 amino acids and a beta-sheet-rich structure. Its tetramer forms as a dimer of dimers with two symmetric funnel-shaped binding sites for thyroxine (T4) that are formed at the dimer–dimer interface. Every TTR tetramer provides four equivalent binding sites for RBP. EF–helix–loop region of each TTR can potentially participate in binding with RBP. However, only two RBPs can bind each TTR tetramer, one on each side due to steric clashes. In the holo-RBP–TTR complex the RBPs interact with subunits of TTR from two different dimers to form a quaternary structure of 'opposite dimer' model.[22,23]

In the resulting models, all domains pack without clashes and visual inspection of the model and the template structure shows good sequence conservation (Figures 3a and b). Each TTR subunit consists of two anti-parallel β-sheet scaffolds, arranged in a *β*-barrel topology with a short α-helix (EF-helix),[22] as shown in Figure 3c. Subunits of the dimer are held together through both hydrogen bond and hydrophobic interactions. The TTR R83s from the two opposing subunits were found to be in close proximity to the R62 of the RBP and this may create electrostatic repulsion and seriously compromise the TTR-RBP stability.

Discussion

FAP is a clinically and genetically heterogenous group of hereditary systemic amyloidosis that can be caused by mutations in TTR, apolipoprotein AI, or gelsolin. In this present study, a heterozygous missense mutation in *TTR* (c.307 C>G) was identified in a five-generation Chinese family with FAP. The Gly83Arg variant is rare, with two prior reports in 2011 and 2012 describing three different Chinese families with FAP.[13,17] Vitreous amyloidosis was the only clinical feature in all affected individuals from these two reports.[13,17] In contrast, the affected individuals in our study had mild polyneuropathy, cardiac amyloidosis, and multiple ocular manifestations, including vitreous opacity, secondary glaucoma, xerophthalmia, dyscoria, and attenuated retinal arteries.

Ocular involvement is reported in approximately 10% of patients with TTR-related FAP, and the incidence of vitreous opacities in different FAP genotype varies from 5.4 to 35%.[24,25] FAP is a clinically heterogenous disorder even in patients with the same *TTR* mutation.[26] However, 100% of affected individuals in all three reports (including this one) describing the TTR Gly83Arg mutation had significant vitreous involvement. The severe visual impairment caused by the dense vitreous opacities found in this family initially improved after an incomplete vitrectomy. However, in 13 eyes of eight patients, visual acuity decreased again several years after the first operation because of reopacification of the residual vitreous in posterior pole, indicating that

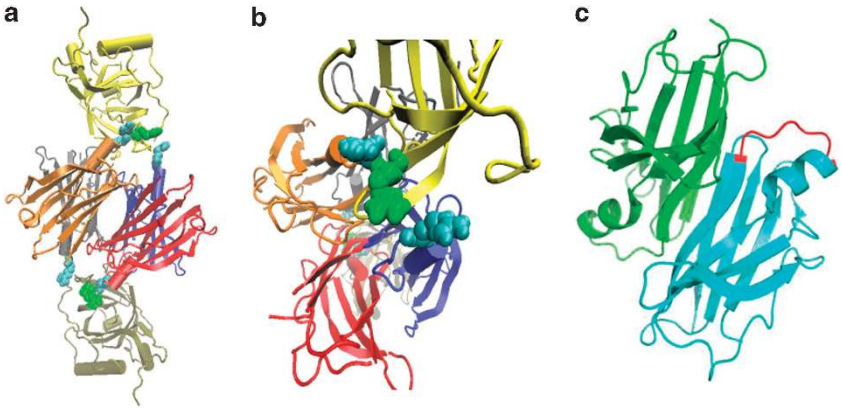

Figure 3 Structure modeling of TTR Gly83Arg and RBP complex. (a) Orthogonal ribbon plots of the modelled complex of the TTR Gly83Arg and RBP. A TTR tetramer was associated with two RBP and each RBP is in contact with two TTRs. The TTR R83 and the RBP R62 are shown as cyan and green space-filled spheres, respectively. (b) A close-up view of the TTR R83 in relation to the RBP R62 in TTR-RBP module. (c) Structure of a TTR Gly83Arg dimer displayed in orthogonal ribbon and the two subunits are labeled in green and cyan, respectively. The EF–helix–loop was highlighted in red.

incomplete vitrectomy with PVD may be a better surgical approach to avoid a second surgery in patients with this mutation. The predilection for fibril formation in the vitreous is unclear; the misfolding of the protein caused by the mutant Gly83 TTR may have a special affinity for the vitreous given the high percentage of individuals with vitreous involvement. Another possibility is this particular mutation causes the RPE to produce mutant TTR that is harder to degrade or forms larger amyloid deposits within the eye than other TTR variants.

In FAP, visual impairment can also be caused by secondary glaucoma induced by amyloid deposits in the trabecular meshwork and Schlemm's canal.[27] The incidence of secondary glaucoma varies from 17 to 24% in FAP. In previous studies, trabeculectomy successfully lowered the IOP.[28] However, in the present study, four patients (IV:4, IV:6, IV:20, and IV:24) continued to have elevated IOP despite medical management, trabeculectomy, and/or cyclophotocoagulation. Patients with TTR Gly83Arg should be monitored regularly for the development of secondary glaucoma.

The sensory-motor polyneuropathy in FAP is usually the predominant clinical feature. In this family, 83% of patients had sensory polyneuropathy with mild numbness or pain of the extremities. In all, 33.3% of patients presented motor dysfunctions such as muscle weakness and atrophy in the distal parts of upper and lower extremities. It suggests TTR Gly83Arg mutation can cause not only predominant ocular lesions but also other systems and organs including polyneuropathy and cardiac amyloidosis.

Currently, there are no treatments available for FAP. Liver transplantation can control disease progression in the nerves;[29] however, liver transplantation require lifelong immunosuppression and are associated with significant morbidity and mortality. In addition, ophthalmic manifestations such as vitreous opacity and glaucoma continue to worsen after liver transplantation because the retinal pigment epithelium continues to produce mutant TTR.[11] Panretinal laser photocoagulation (PRP) was recently reported to prevent the progression of amyloid depositions in the vitreous in two patients with FAP.[30,31] PRP may also be helpful in managing secondary glaucoma associated with FAP as the RPE is the source of mutant TTR in the eye, but further investigations are needed to evaluate the efficacy and safety of PRP in FAP patients with ocular involvement.

The underlying mechanism of the mutation of TTR Gly83Arg in FAP remains to be clarified. We tried to model the structure of the mutation Gly83Arg to explore how the Gly to Arg change will affect the protein structure and function. Crystal structures suggest that the EF–helix–loop region (including residues K80, L82, G83, and I84) of two subunits of the TTR tetramer make significant contribution to the complex formation.[23] The holo-RBP interacts with specific regions of three different subunits of TTR.[23] Residues 82–90 of the EF–helix–loop region of the first subunit participate in the inter-protein interactions.[23,32,33] The mutation of TTR Gly83Arg was located in the EF–helix–loop region, and embedded the key interface for the complex formation. In our model, the TTR R83s from the two opposing subunits were found to be in close proximity to the R62 of the RBP and this may create electrostatic repulsion and seriously compromise the TTR-RBP stability. This explains the instability observed with the TTR Gly83Arg and RBP complex. This is consistent with the previous examination on the role of the EF–helix–loop residues in complex formation with RBP by mutation studies.[32,33]

In conclusion, this study described a Chinese family with FAP due to the TTR variant Gly83Arg. Vitreous opacity is the initial manifestation; other clinical characteristics associated with this mutation include early-onset, secondary glaucoma, polyneuropathy, and cardiac amyloidosis. This disease may be under-diagnosed and FAP should be considered in patients who present with unexplained vitreous opacities. In certain TTR mutations, such as Gly83Arg, vitreous amyloidosis can be the first indication of disease and the first opportunity for diagnosis of FAP may be made by an ophthalmologist. High penetrance and two previous reports of TTR Gly83Arg in China suggest there may be a TTR Gly83Arg mutation hotspot in the Chinese population. Further study of the genotype–phenotype correlations will assist in prognosis counseling as well as increase our understanding of variable disease manifestations.

Summary

What was known before

- Familial amyloid polyneuropathy (FAP) is a group of autosomal dominant inherited disorders and mutations in TTR are the most common cause of FAP.
- The sensory-motor polyneuropathy in FAP is usually the predominant clinical feature, approximately 10% accompanied by vitreous opacities.
- The TTR Gly83Arg variant was reported only in Chinese by two prior studies, in which vitreous amyloidosis was the only clinical feature in all affected individuals.

What this study adds

- A heterozygous TTR Gly83Arg mutation was identified in a five-generation Chinese family with FAP.
- The affected individuals in our study had mild polyneuropathy, cardiac amyloidosis, and multiple ocular manifestations, including vitreous opacity, secondary glaucoma, xerophthalmia, dyscoria, and attenuated retinal arteries.

Conflict of interest

The authors declare no conflict of interest.

Acknowledgements

We thank Dr Sun Zhe for structure modeling of transthyretin, Shi Suozhu from Institute of Nephrology for immunohistochemical study, and Dr Cheng Liuquan from Department of Radiology, Chinese PLA General Hospital, for MRI data acquisition and image interpretation. We are indebted to Dr Zhang Jiatang and Dr Cui Changtai from Department of Neurology, Chinese PLA General Hospital, for neurological diagnosis.

References

1 Ando Y, Araki S, Ando M. Transthyretin and familial amyloidotic polyneuropathy. *Intern Med* 1993; **32**: 920–922.
2 Shin SC, Robinson-Papp J. Amyloid neuropathies. *Mt Sinai J Med* 2012; **79**: 733–748.
3 Hund E, Linke RP, Willing F, Grau A. Transthyretin-associated neuropathic amyloidosis: pathogenesis and treatment. *Neurology* 2001; **56**: 431–435.
4 Plante-Bordeneuve V, Said G. Familial amyloid polyneuropathy. *Lancet Neurol* 2011; **10**: 1086–1097.
5 Monaco HL. The transthyretin-retinol-binding protein complex. *Biochim Biophys Acta* 2000; **1482**: 65–72.
6 Herbert J, Wilocox JN, Pham KT, Fremeau RT, Zeviani M, Dwork A *et al*. Transthyretin: a choroid plexus-specific transport protein in human brain. *Neurology* 1986; **36**: 900–911.
7 Soprano DR, Herbert J, Soprano KJ, Schon EA, Goodman DS. Distribution of transthyretin mRNA in the brain and other extrahepatic tissue in the rat. *J Biol Chem* 1985; **260**: 11793–11798.
8 Dwork AJ, Cavallaro T, Martone RL, Goodman DS, Schon EA, Herbert J. Distribution of transthyretin in the rat eye. *Invest Ophthalmol Vis Sci* 1990; **31**: 489–496.
9 Jaworowski A, Fang Z, Khong TF, Augusteyn RC. Protein synthesis and secretion by cultured retinal pigment epithelia. *Biochim Biophys Acta* 1995; **1245**: 121–129.
10 Cavallaro T, Martone RL, Schon EA, Schon EA, Herbert J. The retinal pigment epithelium is the unique site of transthyretin synthesis in the rat eye. *Invest Ophthalmol Vis Sci* 1990; **31**: 497–501.
11 Hara R, Kawaji T, Ando E, Ohya Y, Ando Y, Tanihara H. Impact of liver transplantation on transthyretin-ralated ocular amyloidosis in japanese patients. *Arch Ophthalmol* 2010; **128**: 206–210.
12 Shi YN, Li J, Hu J, Hu J, Sun LJ, Li HJ *et al*. A new Arg54Gly transthyretin gene mutation associated with vitreous amyloidosis in chinese. *Eye Sci* 2011; **26**: 230–238.
13 Chen LY, Lu L, Li YH, Zhong H, Fang W, Zhang L *et al*. Transthyretin Arg-83 mutation in vitreous amyloidosis. *Int J Ophthalmol* 2011; **4**: 329–331.
14 Long D, Zeng J, Wu LQ, Tang LS, Wang HL, Wang H. Vitreous amyloidosis in two large mainland chinese kindreds resulting from transthyretin variant Lys35Thr and Leu55Arg. *Ophthalmic Genet* 2012; **33**: 28–33.
15 Liu JY, Guo YJ, Zhou CK, Ye YQ, Feng JQ, Yin F *et al*. Clinical and histopathological features of familial amyloidotic polyneuropathy with transthyretin Val30Ala in a chinese family. *J Neuro Sci* 2011; **304**: 83–86.
16 Zhang Y, Deng YL, Ma JF, Zheng L, Hong Z, Wang ZQ *et al*. Transthyretin-related hereditary amyloidosis in a chinese family with TTR Y114C mutation. *Neurodegener Dis* 2011; **8**: 187–193.
17 Xie Y, Zhao Y, Zhou JJ, Wang X. Identification of a TTR gene mutation in a family with hereditary vitreous amyloidosis. *Chin J Med Genet* 2012; **29**: 13–15.
18 Busse A, Sanchez MA, Monterroso V, Alvarado MV, León P. A severe form of amyloidotic polyneuropathy in a Costa Rican family with a rare transthyretin mutation (Glu54Lys). *Am J Med Genet A* 2004; **128A**: 190–194.
19 Strege RJ, Saeger W, Linke RP. Diagnosis and immunohistochemical classification of systemic amyloidoses. Report of 43 cases in an unselected autopsy series. *Virchows Arch* 1998; **433**: 19–27.
20 Jackson E, Bellenger N, Seddon M, Harden S, Peebles C. Ischaemic and non-ischaemic cardiomyopathies–cardiac MRI appearances with delayed enhancement. *Clin Radiol* 2007; **62**: 395–403.
21 Arnold K, Bordoli L, Kopp J, Schwede T. The SWISS-MODEL workspace: a web-based environment for protein structure homology modeling. *Bioinformatics* 2006; **22**: 195–201.
22 Naylor HM, Newcomer ME. The structure of human retinol-binding protein (RBP) with its carrier protein transthyretin reveals an interaction with the carboxy terminus of RBP. *Biochemistry* 1999; **38**: 2647–2653.
23 Zanotti G, Folli C, Cendron L, Alfieri B, Nishida SK, Gliubich F *et al*. Structural and mutational analyses of protein-protein interactions between transthyretin and retinol-binding protein. *FEBS J* 2008; **275**: 5841–5854.
24 Ando E, Ando Y, Okamura R, Uchino M, Ando M, Negi A. Ocular manifestation of familial amyloidotic polyneuropathy type I: long-term follow up. *Br J Ophthalmol* 1997; **81**: 295–298.
25 Zambarakji HJ, Charteris DG, Ayliffe W, Luthert PJ, Schon F, Hawkins PN. Vitreous amyloidosis in alanine 71 transthyretin mutation. *Br J Ophthalmol* 2005; **89**: 773–774.
26 Sandgren O, Drugge U, Holmgren G, Sousa A. Vitreous involvement in familial amyloidotic neuropathy: a genealogical and genetic study. *Clin Genet* 1991; **40**: 452–460.
27 Silva-Araújo AC, Tavares MA, Cotta JS, Castro-Correia JF. Aqueous outflow system in familial amyloidotic polyneuropathy, Portuguese type. *Graefes Arch Clin Exp Ophthalmol* 1993; **231**: 131–135.
28 Kimura A, Ando E, Fukushima M, Koga T, Hirata A, Arimura K *et al*. Secondary glaucoma in patients with familial amyloidotic polyneuropathy. *Arch Ophthalmol* 2003; **121**: 351–356.
29 Yamamoto S, Wilczek HE, Nowak G, Larsson M, Oksanen A, Iwata T *et al*. Liver transplantation for familial amyloidotic polyneuropathy (FAP): a single-center experience over 16 years. *Am J Transplant* 2007; **7**: 2597–2604.
30 Kawaiji T. Retinal laser photocoagulation for familial transthyretin-related ocular amyloidosis. *Nihon Ganka Gakkai Zasshi* 2012; **116**: 1046–1051.
31 Kawaiji T, Ando Y, Hara R, Tanihara H. Novel therapy for transthyretin-related ocular amyloidosis: a pilot study of retinal laser photocoagulation. *Ophthalmology* 2010; **117**: 552–555.
32 Berni R, Malpeli G, Folli C, Murrell JR, Liepnieks JJ, Benson MD. The Ile-84–>Ser amino acid substitution in transthyretin interferes with the interaction with plasma retinol-binding protein. *J Biol Chem* 1994; **269**: 23395–23398.
33 Waits RP, Yamada T, Uemichi T, Benson MD. Low plasma concentrations of retinol-binding protein in individuals with mutations affecting position 84 of the transthyretin molecule. *Clin Chem* 1995; **41**: 1288–1291.